

# A comparative study of bioprinting extrusion nozzles geometries

JC. Gómez Blanco<sup>1</sup>, E. Mancha Sánchez<sup>1</sup>, FM. Sánchez Margallo<sup>1</sup>, JB. Pagador Carrasco<sup>1</sup>

<sup>1</sup>Centro de Cirugía de Mínima Invasión Jesús Usón, Cáceres, España,  
{jcgomez, emancha, msanchez, jpagador}@ccmijesususon.com

## Abstract

*Extrusion bioprinting is an additive manufacturing technology with huge possibilities in the creation of engineered tissues. There are lots of works regarding to this technology and the materials used. Nowadays researches are using computational simulations to study different parameters that can have influence on the cellular survival. In this way we have done Computational Fluids Dynamics (CFD) simulations to check how the extrusion nozzle geometry affects the flow pressure distribution. Results show that variations in geometry will lead to variations in pressure distribution. It is necessary to perform further simulations in future studies with parametric modifications in nozzle geometries to achieve the optimum nozzle geometry which can help cell survive by reducing the pressure.*

## 1. Introduction

Additive manufacturing is a fabrication method created in the 80' and popularised nowadays under the name of 3D printing. This kind of technology works under a simple principle: the creation of an object layer by layer. It means that a certain amount of material is disposed in a defined place in each layer, the consecutive addition of layers creates an 3D object. This fabrication method allows intricate geometry which means the possibility of fabricating objects that conventional manufacturing methods cannot allow.

Bioprinting is the application of 3D printing technologies in health or biology [1-3]. This "type" of 3D printing operates under the same principle as the conventional technology with the particularization of using with cell-laden or cell-compatible materials. Materials used in bioprinting are usually 1) polymers as Polycaprolactone (PCL) or methylcellulose and 2) hydrogels as Alginate or Hyaluronic Acid (HA). In fact, any kind of material can be used for bioprinting as long as they are biocompatible (allow cells to live and proliferate) and biodegradable [4-6]. Many previous works analyse which material is better according to the biological material to be bioprinted [7-9]. In this sense, a proper selection of the biological material is another key point. According to the clinical/medical application different stem cells are used, such as Bone Narrow Stem Cells (BNSCs) in bone scaffolds or Mesenchymal Stem Cells (MSCs) in cartilage regeneration. Cells are very sensitive and need a proper environment and nutrients to live and proliferate [10]. For this reason, a bioprinter must control, at least, temperature, pressure, CO<sub>2</sub> and pH [11].

Although other deposition methods are possible, maybe the most common techniques used in bioprinting are extrusion, inkjet and laser-assisted [12]. Mainly due to cost-effective reasons, the most used technique is the extrusion-based that deposit biomaterials through a customized nozzle [13]. So, these kinds of bioprinters use extrusion heads that are usually formed by a syringe and a needle or a tapered nozzle (conical tip). It is well described in bibliography that the pressure is one of the most important factors that can provoke a low cell survival [8].

Computational simulations are widely extended in calculation of flows through nozzles [14-15]. However, bioprinting related simulations have still room for improvement with only a few research studies [16-17]. For this reason, CFD in bioprinting technology could provide useful data of material flows and help to select the most appropriate hydrogel for the survival of cells.

Hence, the main objective of this work is to compare the pressure in the tip of the tapered nozzle versus the needle through computational fluid simulation for a biocompatible material.

## 2. Methods

### 2.1. Model

Two different models were created and simulated in COMSOL Multiphysics through a 2D axisymmetric model and the Two-Phase Flow (TPF) level set interface. One model is the related to the tapered nozzle and the other is the needle one. The tapered nozzle was modelled by a trapezium of 25 mm of height, 3 mm of the inlet face and 0.2 mm of the outlet face. The needle was modelled by a 15 mm height and 0.2 mm width rectangle and a 2 mm width and 5mm height triangle. The rest of the geometry is the air where the nozzle ejects the material and it is composed by a rectangle and a trapezium.

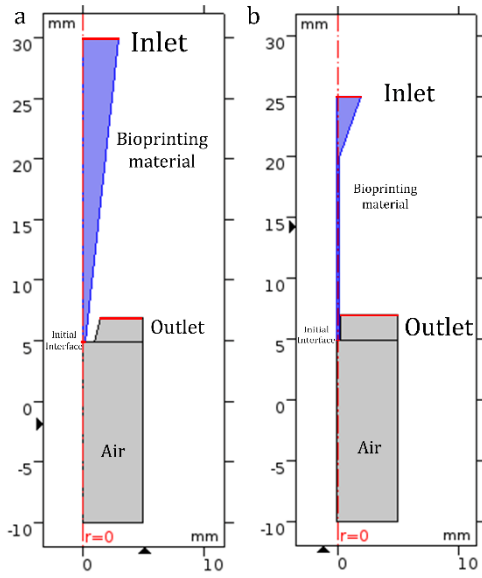


**Figure 1.** Representation of both models: a) is the tapered nozzle and b) is the needle.

## 2.2. Governing equations

Level set (LS) method is a transport equation which is added to incompressible Navier-Stokes equations to track the interface of two immiscible fluids, in this case bioprinting materials and air, these equations are:

$$\rho \frac{\partial u}{\partial t} + \rho(u \cdot \nabla)u = \nabla \cdot [-pI + \mu(\nabla u + \nabla u^T)] + F + \rho g$$

$$\nabla \cdot u = 0$$

where,  $\rho$  is the density,  $u$  is the speed of the fluid,  $p$  denotes the pressure,  $I$  is the identity matrix,  $F$  is all other external forces and  $g$  is the gravity force.

In the level set equation, the bioprinting material is expressed by  $\phi = 0$ , the air is expressed by  $\phi = 1$  and the contour lines of level set is expressed by  $\phi = 0.5$ . The level set equation can be seen as the volume percentage of water in the gas-liquid two-phase flow [18]. Therefore, the migration equation of the gas-liquid interface can be written as follows:

$$\frac{\partial \phi}{\partial t} + u \cdot \nabla \phi = \gamma \nabla \cdot \left( \epsilon_{ls} \nabla \phi + \phi(1 - \phi) \frac{\nabla \phi}{|\nabla \phi|} \right)$$

where  $\phi$  is the contour line of the interface of the gas-liquid two-phase flow,  $\gamma$  is the reinitialization parameter to solve the equation,  $\epsilon$  is the interface thickness controlling parameter. Here, bioprinting material corresponds to the domain where  $\phi < 0.5$ , and air corresponds to the domain where  $\phi > 0.5$ .

## 2.3. Domains

In this model, two different domains were considered. The first domain is related to the nozzle where the hydrogel is placed, and the second domain is the outside of the nozzle,

the air where the biological material is ejected. The material used for the simulation is a mixture of Alginate (1%) and Gelatine (10%) which has a density of  $1455.08 \text{ kg/m}^3$  and a viscosity of  $0.83 \text{ Pa} \cdot \text{s}$ . To make possible a flow, an inlet was placed in the top part of the nozzle with a value of  $1 \text{ mm/s}$ . Also, an outlet condition was set at the top part of the air domain to allow bioprinting material to fill this domain and air to leave. An initial interface boundary condition was placed at the end of the nozzle to define a boundary where the fluid (hydrogel) finishes and the air starts.

## 2.4. Mesh

A 2D triangular mesh was created for the simulations of each model. For better simulations an adaptative mesh refinement was set as can be seen in Figure 2. This creates multiple meshes for segments of the time-dependent simulation. For the tapered nozzle model, the initial triangular mesh has 2892 triangular elements, while the remeshing raise the number of elements up to 5102 in the zone where the interface between both materials is placed. For the needle model, mesh has 2242 triangular elements and as the previous model remeshing raise the number of elements up to 4138.

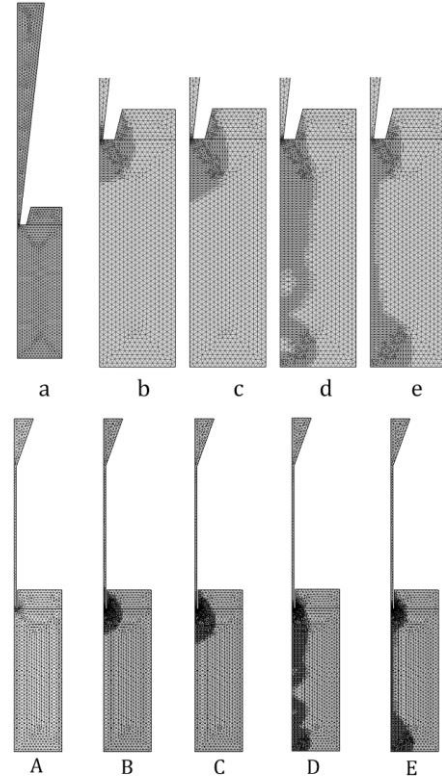


**Figure 2.** Original mesh (a, A) and mesh refinement procedure during the simulations. Lower-case letters correspond to the tapered nozzle model and capital letters correspond to the needle.

## 2.5. Simulation

A 1.5 s simulation, using a 5 ms step, for each model was carried out, composed of two study steps, Phase Initialization and Time Dependent. The Phase Initialization

step solves for the distance to the initial interface  $>, D_{wi}$ . Then the Time Dependent step uses the initial condition for the level set function according to the following expression:

$$\phi_0 = \frac{1}{1 + e^{D_{wi}/\epsilon}}$$

in domains initially filled with bioprinting material and:

$$\phi_0 = \frac{1}{1 + e^{-D_{wi}/\epsilon}}$$

in domains initially filled with air.

For Phase Initialization step a stationary solver was used. A fully coupled solver with a linear direct PARDISO method and a Newton non-linear method was used. For the Time Dependent step a time-dependent solver was used with the non-linear method with a constant Newton damping factor, in this case 1.

### 3. Results and Discussion

#### 3.1. Fluid Volumetric Fraction

The amount of each material is represented by the fluid volumetric fraction. Values 1 means that the 100% of the material is composed by a certain material (not air). Therefore 0 values mean that all the material is air. Figure 3 shows the drop formed at 0.695 s of the simulation done with the tapered nozzle. This time is the first moment when a drop is form and the last moment when the drop is still attached to the nozzle. The interface between the material and air is defined in the figure with a fluid fraction volume of 0.5.

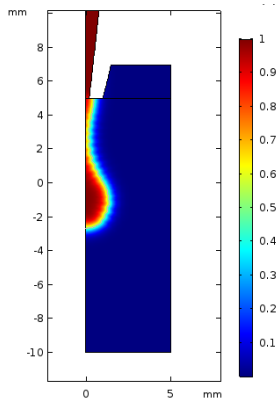


**Figure 3.** Fluid Volumetric Fraction of tapered nozzle model in 0.695 s.

In the total time of tapered nozzle simulation (1.5 s) two drops are formed and felt down.

Figure 4 shows the drop formed at 0.47 s of the simulation done with the needle. At the end of this simulation (1.5 s) four drops where formed but only three of them felt down.

It is clear that the shape of the nozzle has impact on the formation of the drop. In this case, not only the size of the nozzle modifies the drop formation, but the width of the wall affects the size of the drop that can be attached to the needle. Needle has a small wall width (0.15 mm) against the wall of the nozzle (0.8 mm) so, the drop has less contact surface to get attached to, reducing the material needed to fall. In these simulations only drops are formed, meanwhile, when bioprinting a continuous flow is used.

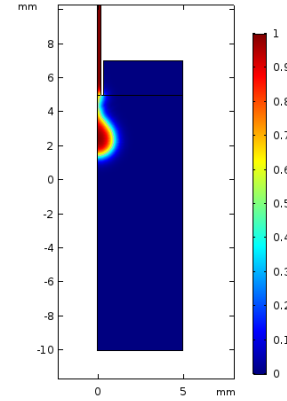


**Figure 4.** Fluid Volumetric Fraction of needle model in 0.47 s.

#### 3.2. Pressures

Pressure plot obtained in the simulations is showed in Figure 5 for both model, the tapered nozzle and needle. These pressures are the obtained at the outlet of the nozzle where the biomaterial leave the nozzle and reach the air. In the nozzle maximum pressure obtained is 105,7 kPa also, it can be seen two losses of pressure corresponding to the moment when the drops felt. In this case only two drops are released from the nozzle. In the needle model the maximum pressure level obtained is 102,6 kPa. In this case, three drops felt. Comparing the pressures from both model it is noted that in the tapered one the pressure is slightly higher than in the needle one.

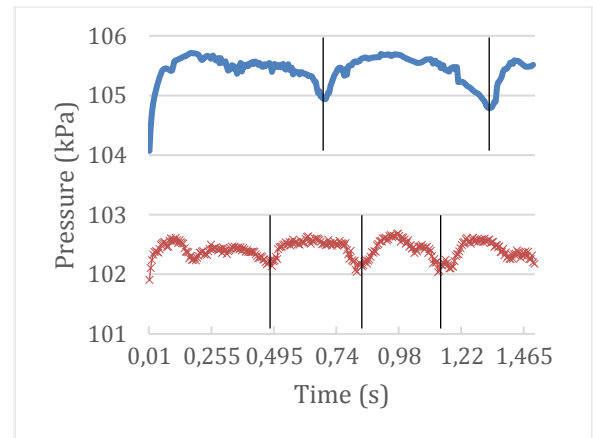


**Figure 5.** Pressure plot of both models. Blue line corresponds to the tapered nozzle, red crosses correspond to needle. Vertical lines show where drops are formed.

Figure 5 shows the pressure at the outlet, but this is not the place where the pressure is maximum on the needle model. The place where the pressure is higher is the beginning of the straight part of the needle as it can be seen in Figure 6. This pressure is three times higher than in the outlet

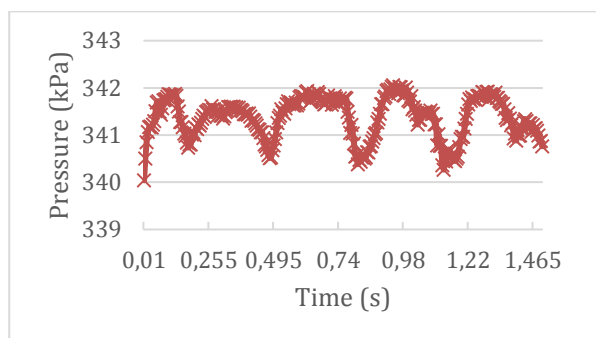


**Figure 6.** Pressure plot of straight interface of the needle.

This study only shows a small time of the whole bioprinting process, longer simulation is required to see how pressure changes along the time. Also, it is needed to study the shear stress on the biomaterial during the extrusion to see if it reaches values that can endanger cellular viability.

#### 4. Conclusions

In this work different computational simulations of the flow of a bioprinting material through two different extrusion bioprinting nozzles have been done. We have checked two important facts, 1) variations on the nozzle geometry provoke a variation in pressure at the tip and 2) Inner geometry of the extrusion nozzle must be studied further due to high pressure changes.

To have a better understanding of the pressure variations in different geometries it is necessary to perform future simulations with parametric modifications in nozzle geometry. Also, it is required to obtain a continuous flow not only a single drop to perform a more realistic simulation of the bioprinting process. Huge amounts of data from simulation will allow to obtain the optimum nozzle tip for a determined bioprinting material and cell used attending to pressure distribution.

#### Acknowledgements

This work was supported by Consejería de Economía e Infraestructuras, Junta de Extremadura. Project number IB16200 "Optimización y mejora de técnicas de bioimpresión para regeneración de cartílago y prótesis vasculares".

#### References

[1] H.-W. Kang, J. J. Yoo, and A. Atala, "Bioprinted Scaffolds for Cartilage Tissue Engineering," *Cartilage Tissue Engineering: Methods and Protocols*, vol. 1340, pp. 981–995, 2015.

[2] Y. D. Hesuan et al., "Design and Implementation of Novel Multifunctional 3D Bioprinter," *3d Printing and Additive Manufacturing*, vol. 3, no. 1, pp. 65–68, 2016.

[3] N. Cubo et al., "3D bioprinting of functional human skin: production and in vivo analysis," *Biofabrication*, vol. 9, no. 1, p. 015006, 2016.

[4] E. M. Ahmed, "Hydrogel: Preparation, characterization, and applications: A review," *Journal of Advanced Research*, vol. 6, no. 2, pp. 105–121, 2015.

[5] Y. He et al., "Research on the printability of hydrogels in 3D bioprinting," *Scientific reports*, vol. 6, p. 29977, 2016.

[6] A. Panwar and L. P. Tan, "Current status of bioinks for micro-extrusion-based 3D bioprinting," *Molecules*, vol. 21, no. 6, 2016.

[7] J. Kim et al., "Current status of threedimensional printing inks for soft tissue regeneration," *Tissue Eng Regen Med* (2016) 13: 636.

[8] L. Ning and X. Chen, "A brief review of extrusion-based tissue scaffold bio-printing," *Biotechnology Journal*, vol. 12, no. 8, 2017.

[9] I. T. Ozbolat and M. Hospodiuk, "Current advances and future perspectives in extrusion-based bioprinting," *Biomaterials*, vol. 76, pp. 321–343, 2016.

[10] B. Alberts et al., *Molecular Biology of the Cell*, fifth edit ed., M. Anderson and S. Granum, Eds. Garland Science, Taylor & Francis Group, LLC, 2008, (ISBN: 978-0-8153-4111-6).

[11] Y. Zhao et al., "The influence of printing parameters on cell survival rate and printability in microextrusion-based 3D cell printing technology," *Biofabrication*, vol. 7, no. 4, pp. 1–11, 2015.

[12] F. Pati et al., Chapter 7- Extrusion bioprinting, *Essentials of 3D Biofabrication and Translation 2015* (ISBN 9780128009727).

[13] I. T. Ozbolat, K. K. Moncal, and H. Gudapati, "Evaluation of bioprinter technologies," *Additive Manufacturing*, vol. 13, pp. 179–200, 2017.

[14] W. Yuan and G. H. Schnerr, "Numerical Simulation of Two-Phase Flow in Injection Nozzles: Interaction of Cavitation and External Jet Formation," *Journal of Fluids Engineering*, vol. 125, no. 6, pp. 963–969, jan 2004.

[15] S. Zekovic, R. Dwivedi, and R. Kovacevic, "Numerical simulation and experimental investigation of gas–powder flow from radially symmetrical nozzles in laser-based direct metal deposition," *International Journal of Machine Tools and Manufacture*, vol. 47, no. 1, pp. 112–123, jan 2007.

[16] J. A. Reid et al., "Accessible bioprinting: adaptation of a low-cost 3D-printer for precise cell placement and stem cell differentiation," *Biofabrication*, vol. 8, no. 2, p. 025017, 2016.

[17] W. Martanto et al., "Fluid dynamics in conically tapered microneedles," *AIChE Journal*, vol. 51, no. 6, pp. 1599–1607, 2005.

[18] COMSOL Multiphysics, "Theory for the Two-Phase Flow Interfaces - CFD Module User's Guide," *Manual*, p. 620, 2014.